

Size effects in the electrical resistivity of polycrystalline nanowires

C. Durkan* and M. E. Welland

*Nanoscale Science Laboratory, Department of Engineering, University of Cambridge, Trumpington Street
CB2 1PZ Cambridge, United Kingdom*

(Received 12 November 1999)

Grain-boundary and surface scattering are known to increase the electrical resistivity of thin metallic films and wires. The length scale at which these produce appreciable effects is of the order of the electronic mean free path. For the well-studied case of thin films, both mechanisms can, in principle, be used to explain the observed thickness dependence on resistivity. In order to evaluate which of these mechanisms is more relevant, we have carried out an experimental study of the width dependence of the resistivity of narrow thin-film polycrystalline gold wires (nanowires), and computed the expected behavior on the basis of both surface and grain-boundary scattering mechanisms independently. We find that the resistivity increases as wire width decreases in a manner which is dependent on the mean grain size and cannot be explained adequately by either model alone. We propose a modification to the well-known model of Mayadas and Shatzkes, incorporating the variation of mean grain size on wire dimensions.

I. INTRODUCTION

The scale of interconnects used in the semiconductor industry is continually shrinking towards dimensions comparable with the electronic mean free path. The electrical transport properties of larger wires (in the diffusive transport regime) are well established, the resistance (Ω) following the simple relationship $\Omega = \rho l/A$, where ρ is the resistivity, and l and A are the sample length and cross-sectional area, respectively. Much smaller wires (in the ballistic transport regime), having dimensions comparable with the Fermi wavelength (λ_F), exhibit discrete resistance values, given by $\Omega \propto 1/\text{Int}[A/\lambda_F^2]$, showing a stepwise variation with size. This is due to the confinement of the electronic wave functions by the surfaces. Transport at this scale is well described using the highly successful Landauer-Büttiker formalism.¹

The intermediate region, where a wire has dimensions of the order of the mean free path is, however, a less well-studied area and is where we turn our attention to in this article. Extensive research has been carried out on extended thin films where only one dimension is confined, and we draw on the same tools used to study those systems in order to understand the effect of an extra degree of confinement, in the form of a wire.

The measurement of size and surface-related resistivity effects in conductors has been an area of considerable interest for the past several decades.²⁻⁵ It is well known that the electrical resistivity of thin metallic films increases once the film thickness decreases below the bulk electronic mean free path. Initial work by Fuchs and Sondheimer^{2,3} (FS theory) attributed this effect to diffuse scattering at the film boundaries, which essentially imposes a restriction on the mean free path, as shown in Fig. 1. As the resistivity is inversely proportional to the mean free path, the resistivity consequently increases. Their analysis consisted of solving the Boltzmann transport equation subject to the condition that at the film surfaces, a proportion of the electron distribution function is independent of direction (diffuse scattering). They found reasonable agreement with experimental results

for thin Al and Sn films. Their work was extended to the case of wires of square,⁶ circular,⁷ and finally arbitrary⁸ cross section, with confinement now in two directions.

A simpler and more flexible approach due to Chambers⁸ and based on using kinetic-theory arguments rather than solving the Boltzmann equation explicitly is the approach we take here. In the context of this type of analysis, the only unknown parameter is p , the proportion of electrons that are specularly reflected at the film surfaces. For several decades, the standard procedure has been to fit experimental data using p as the variable parameter. This has resulted in a variety of values for p , some of which are nonintuitive. Towards the end of the 1960s, significant departures from the FS theory were found.⁹ The situation was partially resolved by theoretical work done by Mayadas and Shatzkes^{10,11} (MS theory), who attributed the enhanced resistivity of thin films to grain-boundary scattering superimposed on the smaller Fuchs size effect. The key to their work lay in the observation that up to film thicknesses of the order 1 μm , the mean film grain diameter is approximately equal to the film thickness, due to the growth mode of thin films. Consequently, as one goes

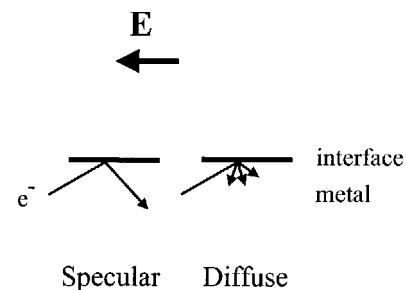


FIG. 1. Illustration of difference between specular and diffuse surface scattering. An incoming electron (e^-) strikes the metal surface and for specular reflection, the component of momentum along the applied field (indicated by E and the arrow) is conserved, whereas for diffuse reflection, it is not and the reflected electron has a random direction of momentum, thus reducing the net current flow.

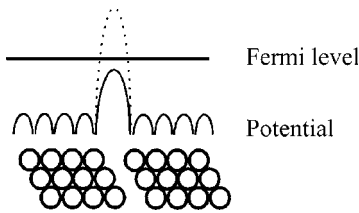


FIG. 2. Illustration of origin of grain-boundary scattering. The circles represent atoms, and the grain boundary consists of a single row of missing atoms. The electric potential is shown above as a solid curve, and the dotted curve shows what the barrier would be like without the image potential.

towards thinner films, the mean grain size decreases, leading to the presence of more grain boundaries and hence an increase in resistivity. In their analysis, the resistivity due to grain-boundary scattering is found to greatly exceed that due to surface scattering. The matter of grain-boundary versus surface scattering remains somewhat unresolved, however, as both the MS and FS theories can actually provide a reasonable fit to experimental data for a variety of cases.^{10,11} Clearly some more exhaustive test is required to distinguish between these two models. The main parameters of the MS theory are ρ and the electron reflection coefficient R , which is the mean probability for an electron to be reflected by a grain boundary. Gold is known to exhibit a high degree of specular reflection from its bare surfaces. From data fits to the MS theory, one can infer $R \sim 0.15$ for Al, and values measured by scanning tunneling microscopy (STM) potentiometry for R for single grain boundaries in Au yield R from 0.4 to as high as 0.9.¹² We have previously reported a value of 0.9 for a single grain boundary in gold.¹³ One can estimate R quite readily by assuming that the grain boundary is equivalent to a missing row of atoms, and consequently the electronic barrier height is reduced significantly below the vacuum level due to the image potential, as illustrated in Fig. 2. Using the WKB method¹⁵ we obtain a value of $R = 0.85$ for gold at the Fermi level.

II. RESULTS

In order to evaluate which model is more appropriate, we have fabricated a series of Au wires of thickness 20 nm, width ranging from 15 to 80 nm, and length 500 nm, and measured the resistivity from four-terminal resistance measurements. The wires were prepared by a process involving both optical and electron-beam lithography. A Si substrate with a well-defined oxide layer of 18.7 nm thickness is spin-coated with AZ 5214 photoresist, which is then exposed to ultraviolet light through a chromium (Cr) mask, using a proximity aligner at a gap of 1 μm . After development, a 1-nm Cr seed layer followed by a 20-nm Au layer is then evaporated onto the sample and the nondeveloped areas lifted off, leaving the large patterns for connection to external testing equipment. This sample is then spin-coated with a layer of low- and then high-molecular-weight poly-methyl methacrylate (PMMA), and the nanowire plus several of the interconnects are patterned by electron-beam lithography. After development, gold is evaporated onto the sample to 20 nm thickness at a base pressure of 10^{-6} mbar following deposition of a 1-nm-thick Cr seed layer, and a final lift-off

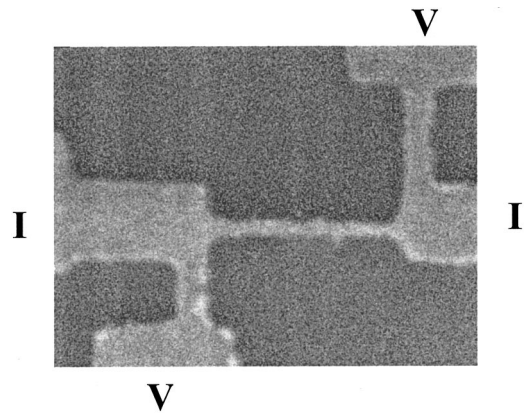


FIG. 3. Electron micrograph of a 45-nm-wide, 20-nm-thick, 500-nm-long gold nanowire showing the current input (I) and voltage measurement (V) points.

process leaves the wire plus interconnects behind on the substrate. The interconnects are bonded with Al wires for connection to external testing equipment. After bonding and before testing, the wires were annealed at 350 $^{\circ}\text{C}$ for 12 h, to reduce the background impurity scattering from defects and impurities.¹⁶ Figure 3 shows a scanning electron microscope (SEM) image of a 45-nm wide wire to illustrate the geometry used. The four-terminal resistance was measured using a computer controlled Keithley 2400 source/meter. Due to the unfavorable effects of Joule heating and electromigration-induced failure^{13,14} in such narrow wires, we always kept the current below 50 μA during testing. For each size of wire, the resistivity of at least four wires was measured and averaged. The deviation was typically $\pm 0.5 \mu\Omega \text{ cm}$ (of the order 7–8%). All of the measurements were performed at room temperature, so electron-phonon scattering will contribute to the background resistance.

A plot of the measured resistivity as a function of the wire width is shown in Fig. 4 (open triangles), from which we can see that the resistivity starts to increase once the wire width decreases below about 45–50 nm. Both electron microscopy and scanning tunneling microscopy revealed that the mean grain size in our films after annealing was of the order 40 nm. Although we had previously reported that there was no size dependence on resistivity,^{13,14} in those cases there had been no anneal and the mean grain size was of the order 20 nm. Our data from these wires is included in Fig. 4 (filled circles). Thus the experimental observations requiring an explanation are (a) the width dependence on the resistivity of narrow wires and (b) the dependence on the mean grain size.

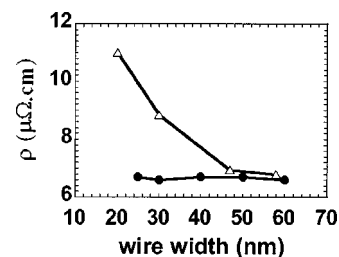


FIG. 4. Measured dependence of resistivity on wire width for a mean grain size of 20 nm (filled circles) and 40 nm (triangles).

III. DISCUSSION

Assuming that the surface scattering (FS term) and grain-boundary scattering (MS term) terms can be described by relaxation times τ_{FS} and τ_{MS} , we can estimate the overall resistivity simply by calculating both terms separately and combining using Mathiessen's rule such that the total resistivity is described by a combined relaxation time, $\tau = (1/\tau_{FS} + 1/\tau_{MS})^{-1}$. The effect of background scattering must then be considered separately, because in the presence of background and surface/grain-boundary scattering, Mathiessen's rule is not satisfied. As we are only interested

in the relative importance of surface and grain-boundary scattering, this is of little consequence to our analysis.

Following the approach of Chambers⁸ we have calculated the surface-scattering component of resistivity for a wire of rectangular cross section. In our analysis, the electronic mean free path is λ , the proportion of electrons specularly reflected from the surface is p , the wire width and thickness are w and h , respectively, the mean grain diameter is D_{50} , and the grain-boundary reflection coefficient is R . Insofar as a mean free path for polycrystalline films can be defined,¹⁷ it is of the order 40 nm for gold.¹⁸ We obtain for the size-dependent component of resistivity

$$\begin{aligned} \frac{\rho_0}{\rho} = & \frac{3}{4\pi h w} \int_{-h/2}^{h/2} dy \int_{-w/2}^{w/2} dx \int_{-\pi + \arctan(w/h)}^{\arctan(-w/h)} d\varphi \int_0^\pi \sin(\theta) \cos^2(\theta) \left[\frac{\exp\left(-\frac{w}{2\lambda \cos(\theta) \cos(\phi)}\right)}{1 - p \exp\left(\frac{w}{-2\lambda \cos(\theta) \cos(\phi)}\right)} \right] d\theta \\ & + \frac{3}{4\pi h w} \int_{-h/2}^{h/2} dy \int_{-w/2}^{w/2} dx \int_{\arctan(-w/h)}^{\arctan(w/h)} d\varphi \int_0^\pi \sin(\theta) \cos^2(\theta) \left[\frac{\exp\left(-\frac{h}{2\lambda \cos(\theta) \cos(\phi)}\right)}{1 - p \exp\left(\frac{h}{-2\lambda \cos(\theta) \cos(\phi)}\right)} \right] d\theta, \end{aligned} \quad (1)$$

where ρ_0 is the bulk resistivity value.

We have numerically evaluated this and the result is plotted in Fig. 5 using a value for p of 0.5 (Au has a high degree of specular reflection⁵) and a film thickness of 20 nm. The extra degree of confinement in a wire essentially adds an offset onto the resistivity above that expected for just one degree of confinement (extended thin film). The calculation clearly shows that the resistivity should only start increasing significantly once the wire width decreases below 25 nm, at odds with our experimental observation. Even if we assume $\lambda = 70$ nm, we calculate that the resistivity will start increasing at a wire width of about 50 nm, but will then increase much more rapidly than experimentally observed. Consequently, using the FS model alone, we cannot explain the

width or the grain-size dependence of the resistivity, so we must now turn to the MS model.

From the MS model, the grain-boundary component of resistivity is given by

$$\frac{\rho_0}{\rho} = 3 \left[\frac{1}{3} - \frac{\alpha}{2} + \alpha^2 + \alpha^3 \ln \left(1 + \frac{1}{\alpha} \right) \right], \quad (2)$$

where

$$\alpha = \frac{\lambda}{D_{50}} \frac{R}{1-R}.$$

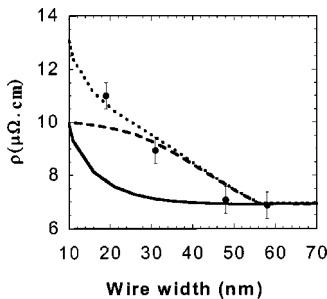


FIG. 5. Calculated dependence of resistivity on wire width (solid curve) based on Fuchs-Sondheimer surface scattering, Mayadas-Shatzkes grain-boundary scattering incorporating the grain size distribution modification (dashed curve), and the combination of both terms calculated using Mathiessen's rule (dotted curve). The points are the measured values from Fig. 4.

In the absence of any dependence of the mean grain size on the wire width, the MS component will be a constant, and the combined resistivity will be dominated by the FS component. The grain size distribution in polycrystalline thin films is known to follow a log-normal distribution.¹⁹ Equation (2) is arrived at by assuming a Gaussian distribution of grain sizes for mathematical simplicity. We propose to modify Eq. (2) to account for the variation in mean film grain size as a function of the linewidth. The rigorous approach would be to incorporate this distribution in the original Boltzmann equation and then find a solution to it, but our aim is only to make a first-order correction to the MS theory in order to explain the observed trends. As the mean grain size follows a simple log-normal distribution, we can analytically estimate the effective grain size distribution as a function of the linewidth. The average distance between grain boundaries is given as

$$D_{\text{eff}} = \frac{\frac{\pi}{4} \int_w^{\infty} f(D) D \frac{D-w}{w} dD}{\int_w^{\infty} f(D) \frac{D-w}{w} dD},$$

where

$$f(D) = \frac{1}{\sigma D \sqrt{2\pi}} \exp \left\{ - \left[\frac{1}{\sqrt{2}\sigma} \ln \left(\frac{D}{D_{50}} \right) \right]^2 \right\}. \quad (3)$$

Here, σ is the log-normal standard deviation of the grain diameters. From the distribution of grain sizes as measured by STM, we find that it can be fitted to a log-normal distribution, with a value for σ of 0.2, reflecting the narrow distribution of grain sizes in our films. From Eq. (3), we calculate that on average the mean distance between grain boundaries (D_{eff}) actually decreases as the wire width (w) decreases, in the range $0.5D_{50} < w < 1.3D_{50}$, reaching plateaux above and below those limits. Therefore the MS theory *does* predict a size dependence on resistivity for polycrystalline thin film wires. Experimentally we find from an analysis of grain sizes (from atomic force microscopy data) that the apparent grain size does indeed decrease with decreasing wire width.

In Fig. 5, we plot the resistivity calculated in this way for a mean film grain size of 40 nm, assuming $R=0.9$. The resistivity reaches a plateau at a wire width of about 60 nm or $1.5D_{50}$ as thereafter, the wire becomes polycrystalline rather than bamboolike, and the average distance between grain boundaries will just be D_{50} . We see that this modified MS theory predicts the resistivity should start increasing ap-

preciably below a wire width of about 50 nm, in good agreement with our data, and should level off below a width of about 30 nm. For the case of a mean grain size of 20 nm, this model predicts that the resistivity should only start increasing at a wire width of about 25 nm, in agreement with our results which showed no width dependence for wires in the size range 25–60 nm. As both scattering mechanisms are occurring simultaneously, to obtain the overall resistivity, we should combine both the FS and modified MS terms using Mathiessen's rule. This is shown as the dotted curve in Fig. 5. We see that the combination of both terms produces a width dependence which is in good agreement with our data, for the following parameters: $\lambda=40$ nm, $D_{50}=40$ nm, $\sigma=0.2$, $p=0.5$, and $R=0.9$. This leads us to the following conclusions regarding polycrystalline wires with dimensions comparable to the electronic mean-free path: First, when the wire width is comparable to the mean film grain size, grain-boundary scattering is the dominant source of increased resistivity. Second, when the wire width is below approximately 0.5 times the mean film grain size, surface scattering becomes important, approaching the same order of magnitude as grain-boundary scattering as the width decreases.

CONCLUSION

We have carried out a study of the width dependence of the resistivity of narrow thin-film polycrystalline gold wires, and computed the expected behavior on the basis of both surface and grain-boundary scattering mechanisms independently. We find that the experimental results can be explained by a combination of both mechanisms if we include the variation of the effective mean grain size on wire width.

*Author to whom correspondence should be addressed.

¹See, for instance S. Datta, *Electronic Transport in Mesoscopic Systems* (Cambridge University Press, Cambridge, 1995).

²K. Fuchs, Proc. Cambridge Philos. Soc. **34**, 100 (1938).

³E. H. Sondheimer, Adv. Phys. **1**, 1 (1952).

⁴N. Koshida, S. Watanuki, K. Yoshida, K. Endo, M. Komuro, and N. Atoda, Jpn. J. Appl. Phys., Part 1 **31**, 4483 (1992).

⁵W. F. Egelhof, Jr., P. J. Chen, C. J. Powell, D. Parks, G. Serpa, R. D. McMichael, D. Martien, and A. E. Berkowitz, J. Vac. Sci. Technol. B **17**, 1702 (1999).

⁶D. K. C. MacDonald and K. Sarginson, Proc. R. Soc. London, Ser. A **203**, 223 (1950).

⁷R. B. Dingle, Proc. R. Soc. London, Ser. A **201**, 545 (1950).

⁸R. G. Chambers, Proc. R. Soc. London, Ser. A **202**, 375 (1950).

⁹A. F. Mayadas, J. Appl. Phys. **39**, 4241 (1968).

¹⁰A. F. Mayadas, M. Shatzkes, and M. Janak, Appl. Phys. Lett. **14**,

345 (1969).

¹¹A. F. Mayadas and M. Shatzkes, Phys. Rev. B **1**, 1382 (1970).

¹²M. A. Schneider, M. Wenderoth, A. J. Heinrich, M. A. Rosentretter, and R. G. Ulbrich, J. Electron. Mater. **26**, 383 (1997).

¹³C. Durkan, M. A. Schneider, and M. E. Welland, J. Appl. Phys. **86**, 1280 (1999).

¹⁴C. Durkan and M. E. Welland, Ultramicroscopy **82**, 125 (2000).

¹⁵See, for instance, C. J. Chen, *Introduction to Scanning Tunneling Microscopy* (Oxford University Press, New York, 1993).

¹⁶M. C. Hersam, M. Phil. thesis, University of Cambridge (1997).

¹⁷J. Vancea, G. Reiss, and H. Hoffmann, Phys. Rev. B **35**, 6435 (1987).

¹⁸See, for instance, N. W. Ashcroft and N. D. Mermin, *Solid State Physics* (Saunders College, Philadelphia, 1976).

¹⁹Y.-C. Joo and C. V. Thompson, J. Appl. Phys. **76**, 7339 (1994).